Electronic Supplementary Material (ESI) for Materials Chemistry Frontiers.

Halogen-induced planar defects in Cu catalyst for ammonia electrosynthesis at an ampere-level current density

Yan Wang,[a,#] Shuai Xia,[a,#] Jianfang Zhang,[a,*] Ashok Kumar Ummireddi,[b] Zhengyuan Li,[b] Xu Yuan,[a] Cuiping Yu,[a] Yong Zhang[a,c], Jingjie Wu,[b,*] and Yucheng Wu[a,c,d,*]

[a]School of Materials Science and Engineering, Hefei University of Technology, Hefei 230009, China

[b]Department of Chemical and Environmental Engineering, University of Cincinnati, Cincinnati, OH 45221, United States

[c]China International S&T Cooperation Base for Advanced Energy and Environmental Materials & Anhui Provincial International S&T Cooperation Base for Advanced Energy Materials, Hefei University of Technology, Hefei 230009, China

[d]Key Laboratory of Advanced Functional Materials and Devices of Anhui Province, Hefei University of Technology, Hefei 230009, China

[#]These authors contributed equally.

*Correspondence:
jfzhang@hfut.edu.cn; wu2jj@ucmail.uc.edu; ycwu@hfut.edu.cn

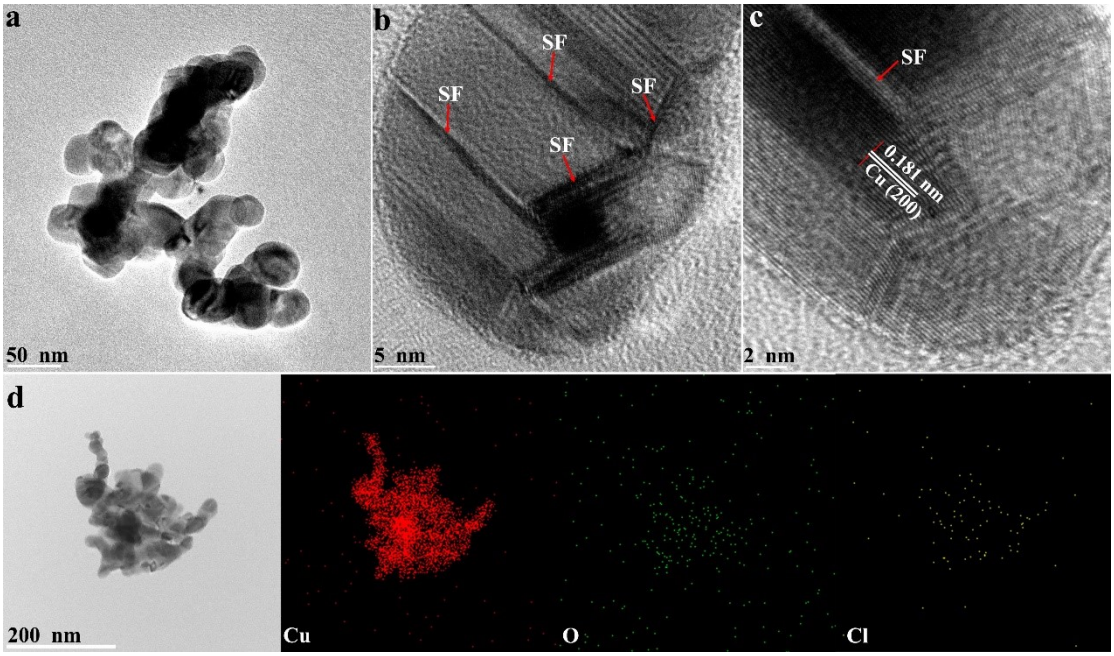

Figure S1. (a) TEM, (b, c) HRTEM and (d) EDX elemental mapping images of Cu-Cl catalyst.

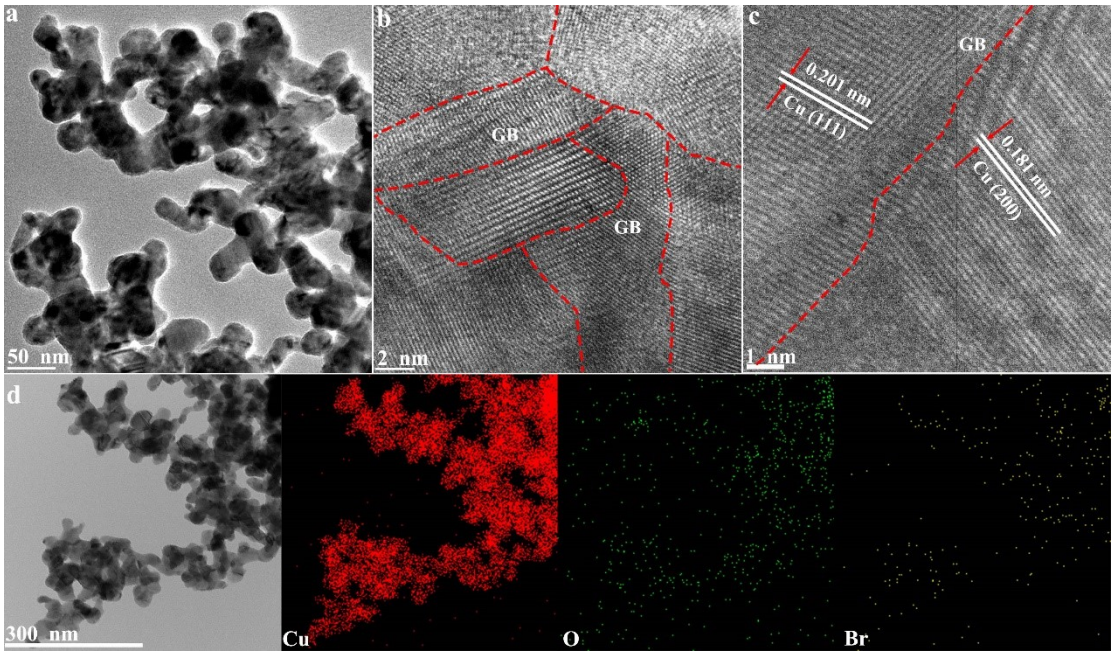

Figure S2. (a) TEM, (b, c) HRTEM and (d) EDX elemental mapping images of Cu-Br catalyst.

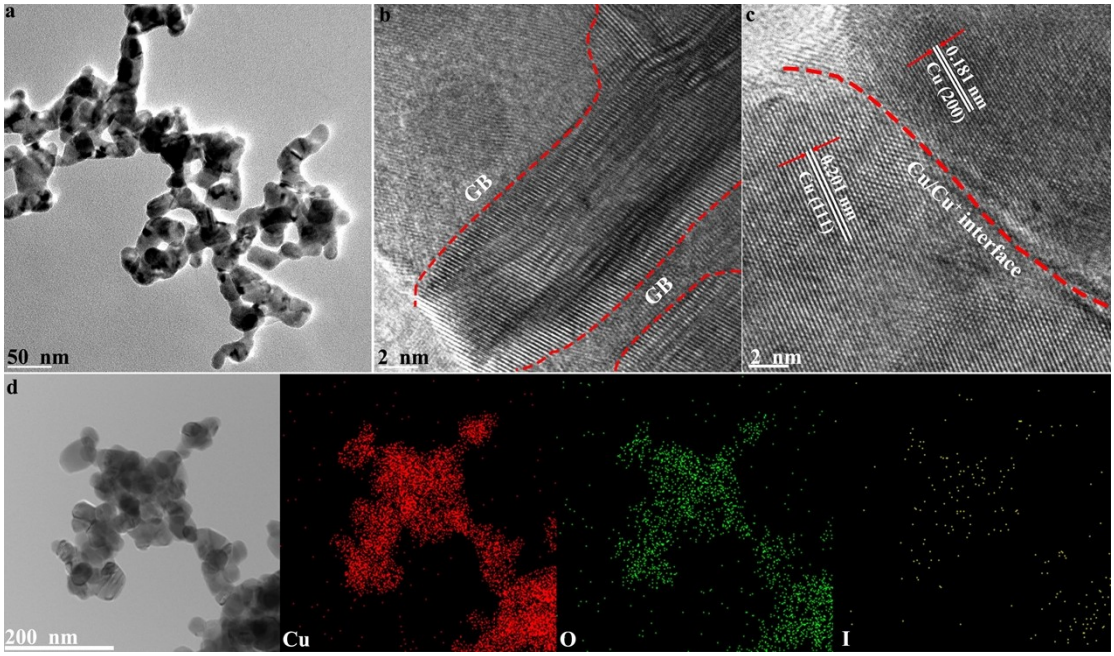

Figure S3. (a) TEM, (b, c) HRTEM and (d) EDX elemental mapping images of Cu-I catalyst.

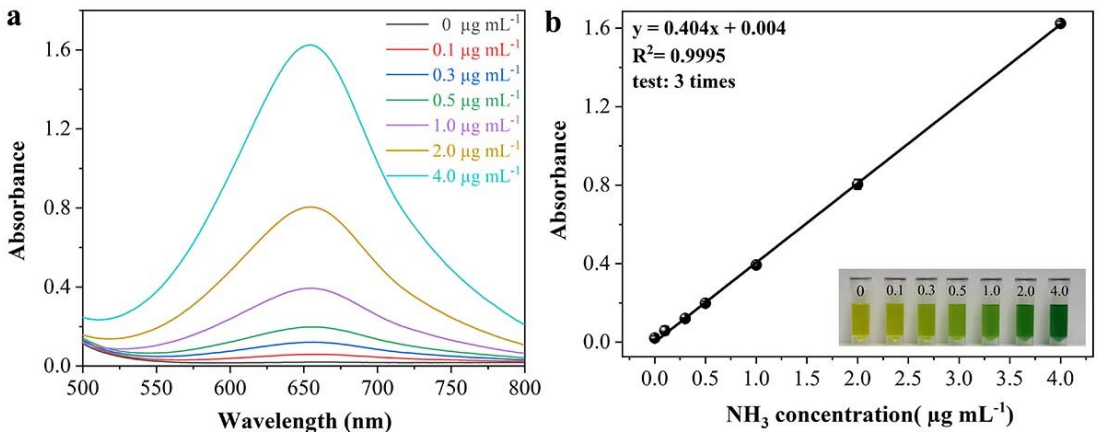

Figure S4. (a) UV-Vis spectra and (b) corresponding standard curve of various concentrations of NH_3.

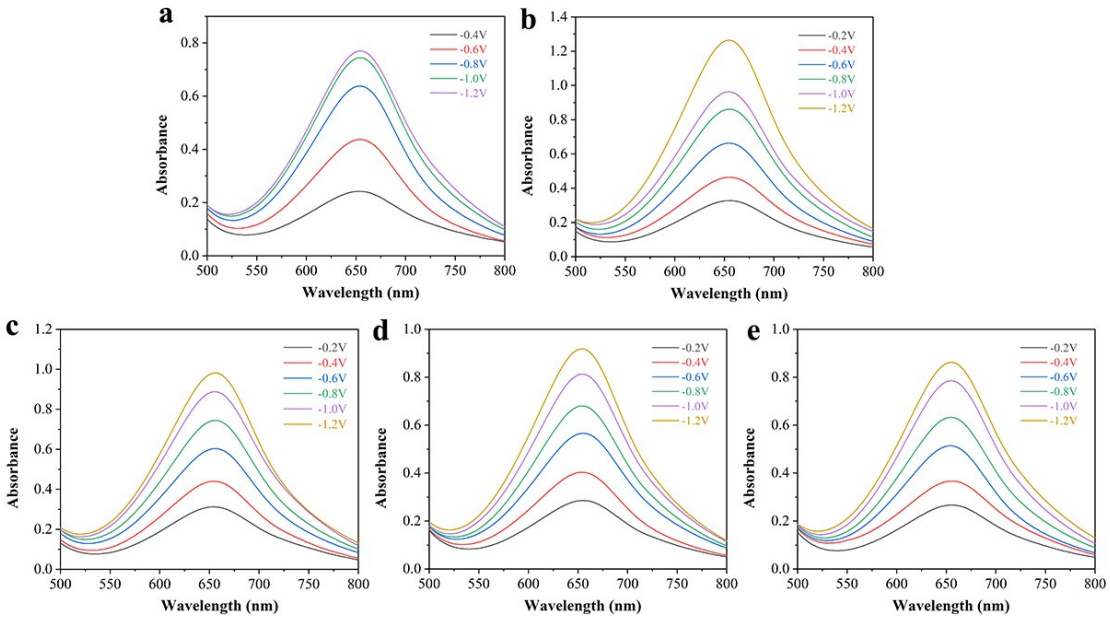

Figure S5. UV-Vis spectra of Cu-X electrodes under different potentials. (a) Cu, (b) Cu-F, (c) Cu-Cl, (d) Cu-Br, and (e) Cu-I.

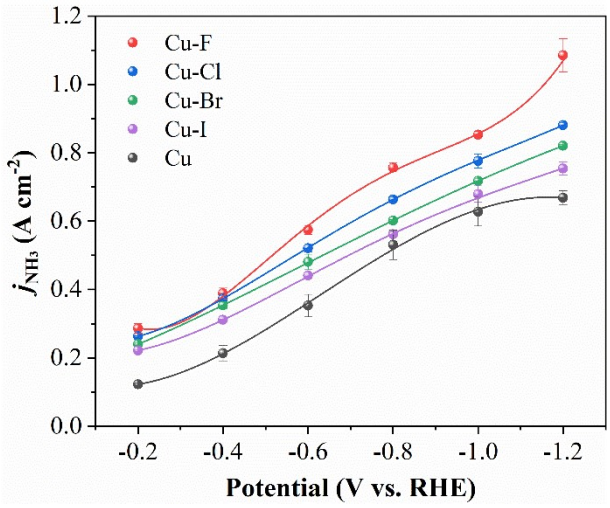

Figure S6. The partial current density of NH_3 generated on different electrodes.

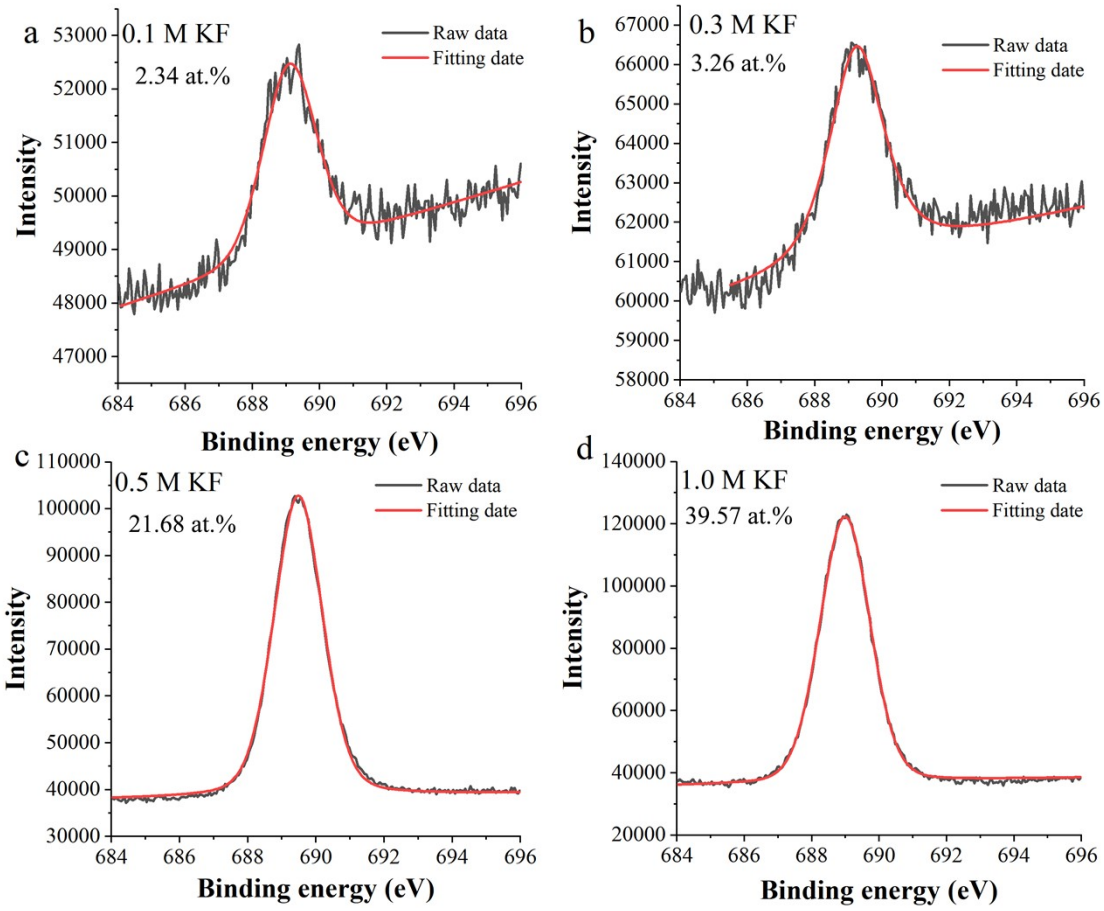

Figure S7. XPS spectra of F 1s in the Cu-F electrode prepared by different concentrations of KF. (a) 0.1 M, (b) 0.3 M, (c) 0.5 M, and (d) 1.0 M.

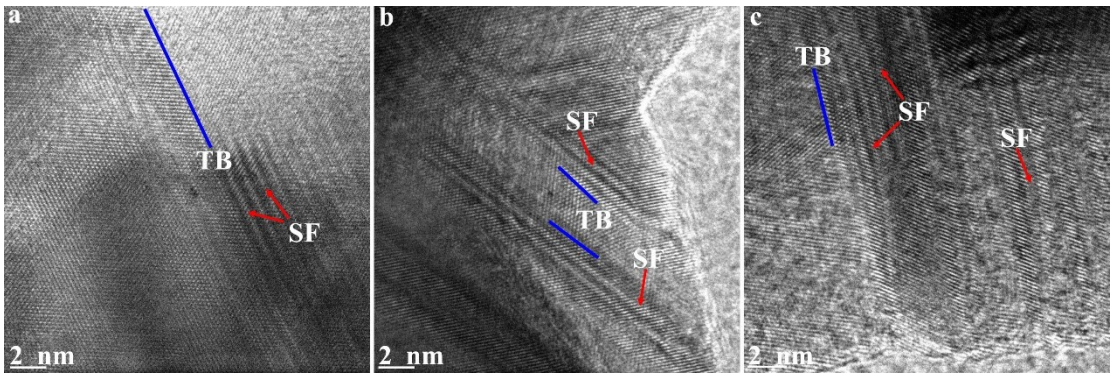

Figure S8. HRTEM images of different Cu-F electrodes prepared by (a) 0.1 M KF, (b) 0.3 M KF, and (c) 1.0 M KF.

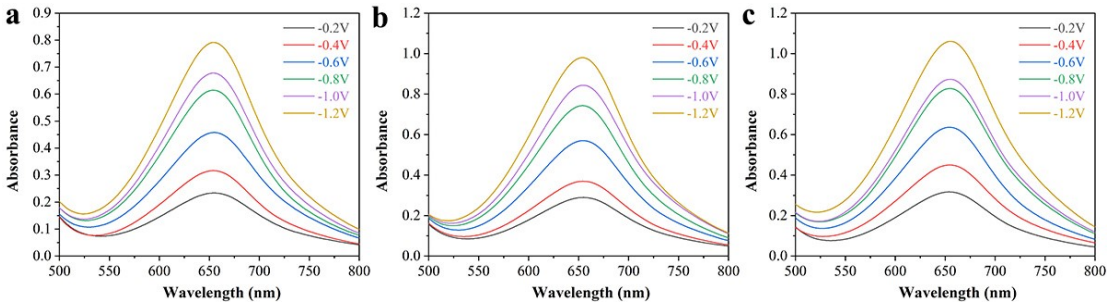

Figure S9. UV-Vis spectra of NH_3 generated on Cu-F electrode in different concentrations of KF. (a) 0.1 M, (b) 0.3 M, and (c) 1.0 M.

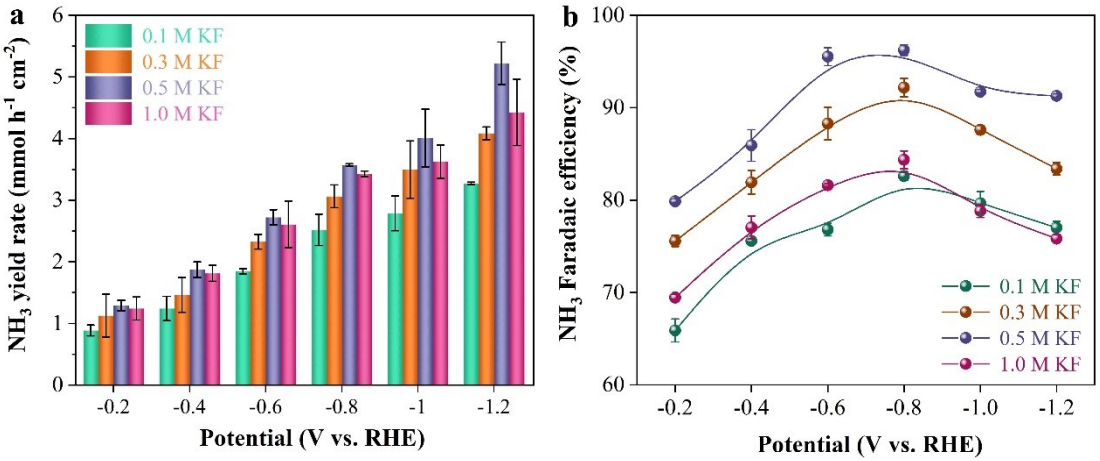

Figure S10. (a) The yield rates and (b) FEs of NH_3 generated on Cu-F electrode in different concentrations of KF.

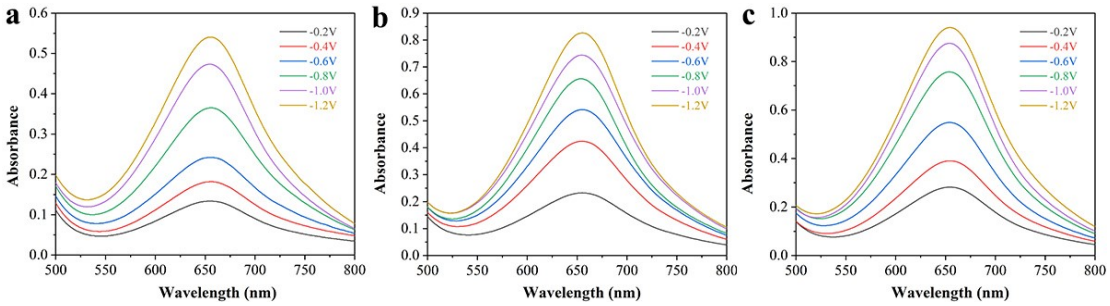

Figure S11. UV-Vis spectra of NH_3 generated on Cu-F electrode in different concentrations of KNO_3. (a) 0.05 M, (b) 0.1 M, and (c) 0.5 M.

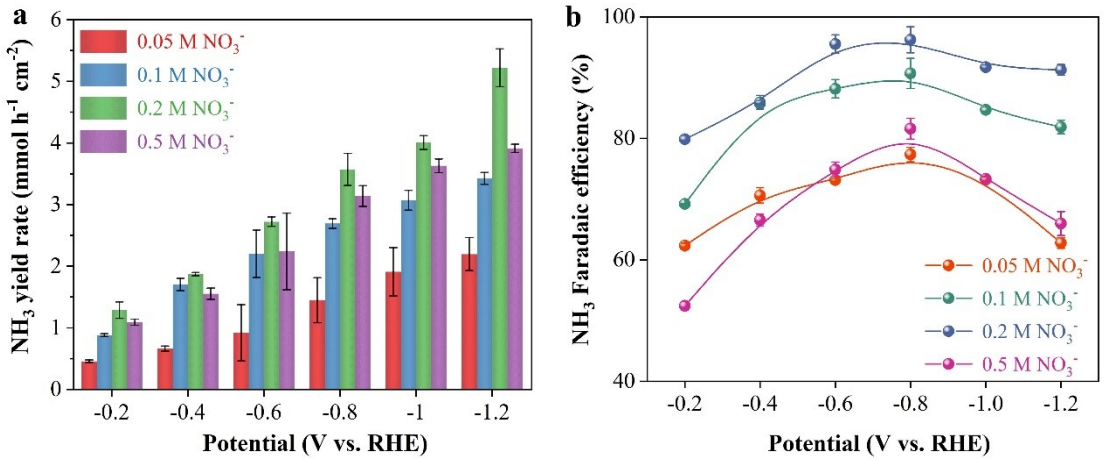

Figure S12. (a) The yield rate and (b) FE of NH_3 generated on Cu-F electrode in different concentrations of KNO_3.

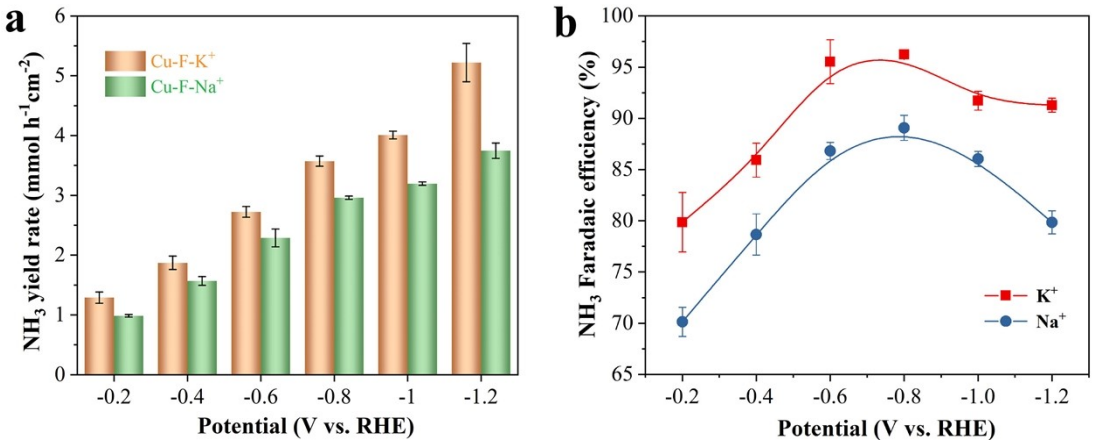

Figure S13. Comparison of NO_3^-RR performance of Cu-F electrode between KNO_3 and $NaNO_3$ electrolyte. (a) The yield rate and (b) FE of NH_3.

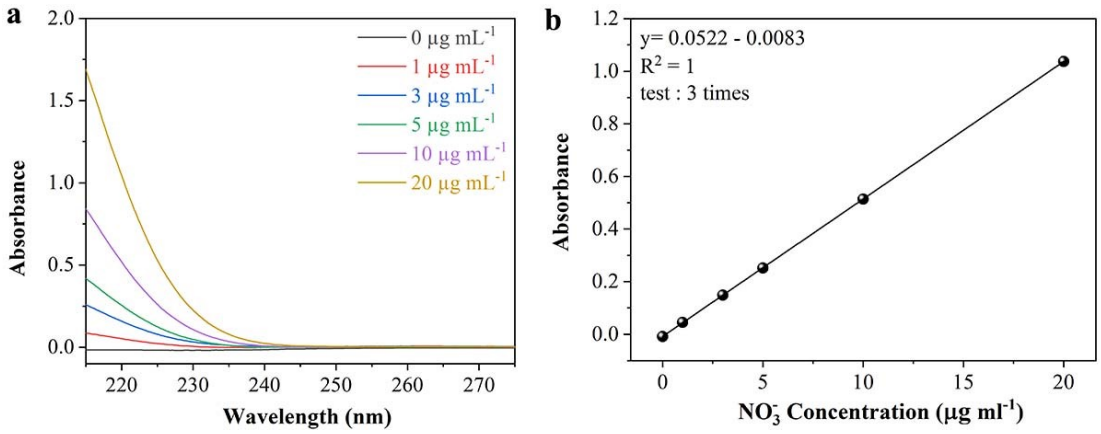

Figure S14. (a) UV-Vis spectra and (b) corresponding standard curve of various concentrations of NO_3^-.

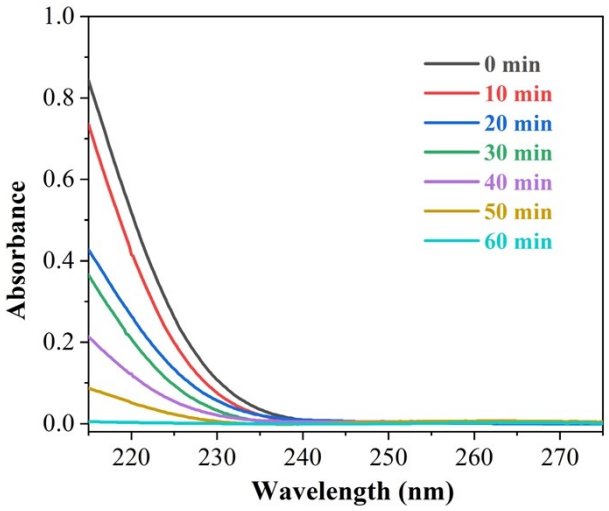

Figure S15. UV-Vis spectra of NO_3^- in the electrolyte at different reaction duration.

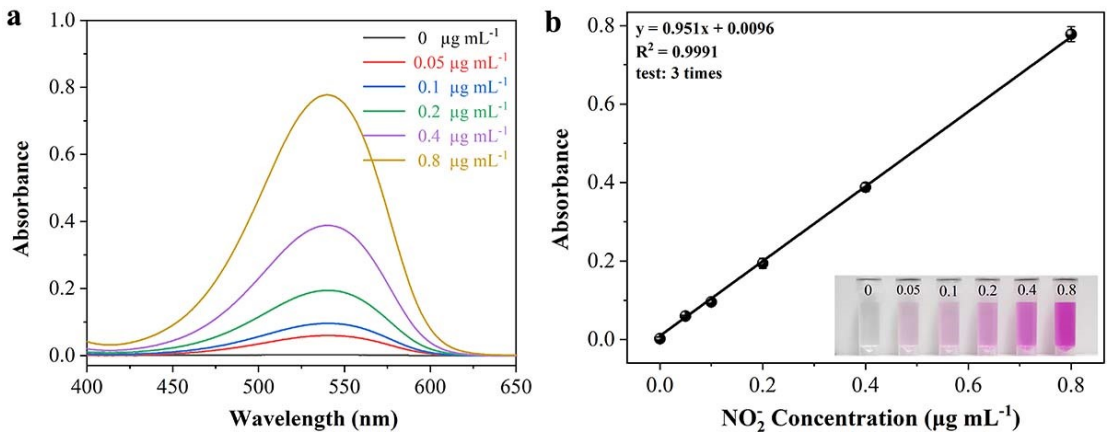

Figure S16. (a) UV-Vis spectra and (b) corresponding standard curve of various concentrations of NO_2^-.

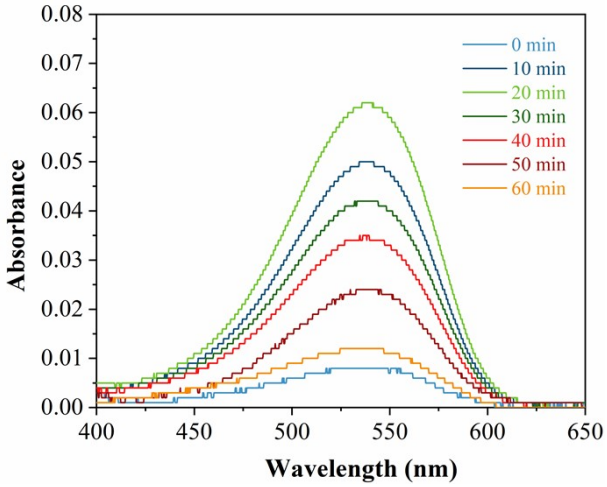

Figure S17. UV-Vis spectra of NO_2^- in the electrolyte at different reaction duration.

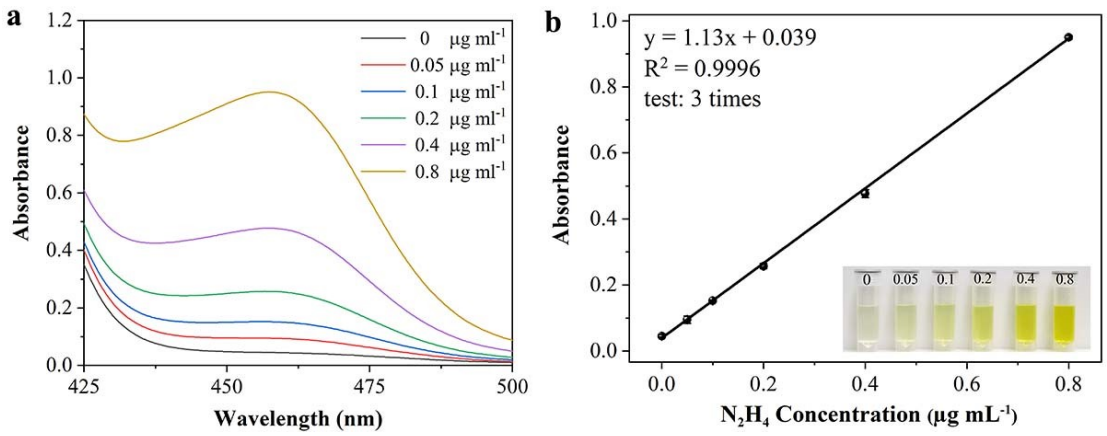

Figure S18. (a) UV-Vis spectra and (b) corresponding standard curve of various concentrations of N_2H_4.

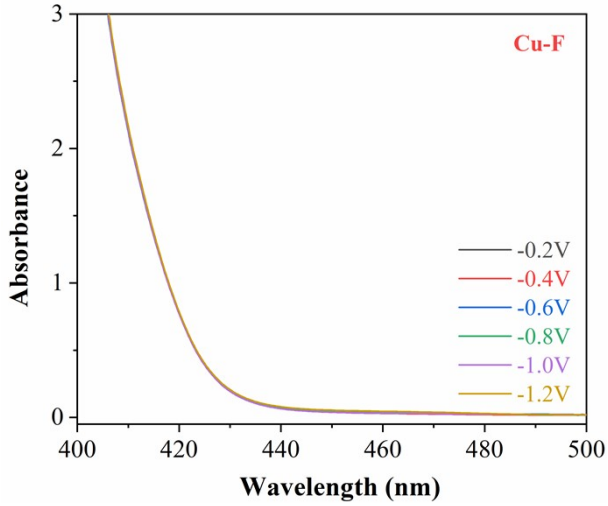

Figure S19. UV-Vis spectra of N_2H_4 produced on Cu-F at different potentials.

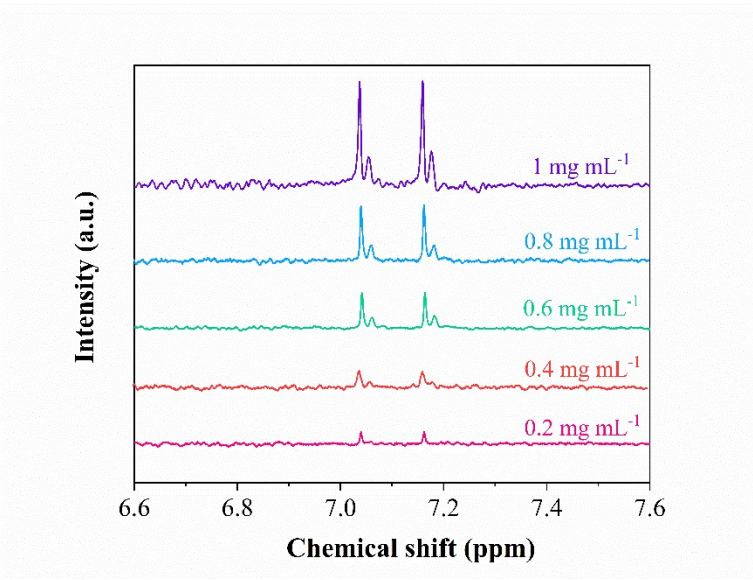

Figure S20. ^{1}H NMR spectra of $^{15}NH_4^+$ with different standard concentrations.

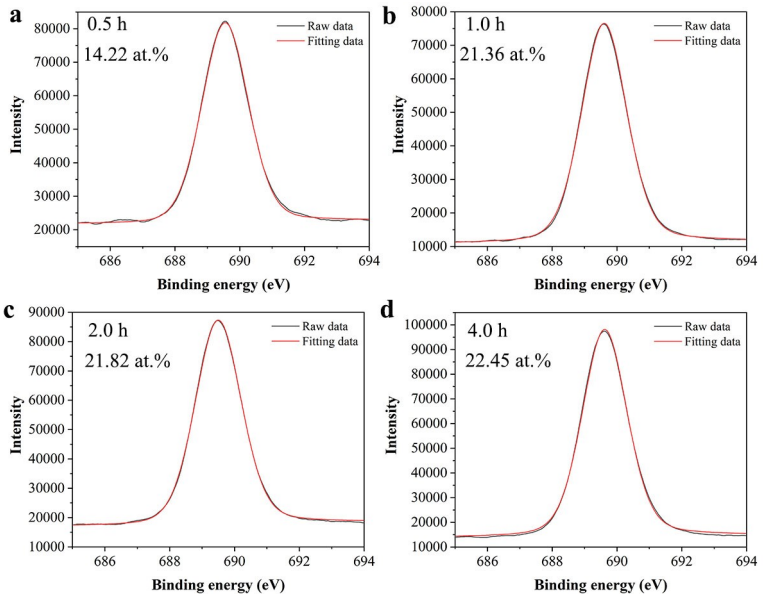

Figure S21. XPS spectra of F 1s in the Cu-F electrode at different reaction times.

Table S1. The calculated grain sizes of different Cu-X and Cu catalysts.

samples	K	λ	β (FWHM)	2θ	D
Pure Cu	0.89	0.15405	0.247	43.25	43.7
Cu-F	0.89	0.15405	0.291	43.38	29.1
Cu-Cl	0.89	0.15405	0.319	43.30	26.5
Cu-Br	0.89	0.15405	0.401	43.40	21.1
Cu-I	0.89	0.15405	0.383	43.27	22.1